metals

MDPI

Article

The Corrosion Inhibition Effect of Triazinedithiol Inhibitors for Aluminum Alloy in a 1 M HCl Solution

Qian Zhao [1], Tiantian Tang [1], Peilin Dang [1], Zhiyi Zhang [2] and Fang Wang [1,*]

[1] College of Chemistry & Pharmacy, Northwest A&F University, Xinong Road No. 22, Yangling 712100, China; qianzhao-0918@163.com (Q.Z.); tangtiantian1020@foxmail.com (T.T.); dangpeilin1117@nwsuaf.edu.cn (P.D.)

[2] College of Information Engineering , Northwest A&F University, Xinong Road No. 22, Yangling 712100, China; zhangzhiyi@nwsuaf.edu.cn

* Correspondence: wangfang4070@nwsuaf.edu.cn; Tel.: +86-29-870-92226

Academic Editor: Hugo F. Lopez

Received: 5 January 2017; Accepted: 3 February 2017; Published: 5 February 2017

Abstract: Two environmental friendly triazinedithiol inhibitors 6-diallylamino-1,3,5-triazine-2,4-dithiol monosodium (DAN) and 6-dibutylamino-1,3,5-triazine-2,4-dithiol monosodium (DBN) were synthesized and their corrosion inhibition for aluminum alloy in a 1 M HCl solution was studied using weight loss methods, electrochemical measurements, and scanning electron microscopy (SEM) techniques. The inhibition efficiency of both DAN and DBN improved with increases in inhibitor concentration but decreased with increases in temperature. Results from potentiodynamic polarization and EIS showed that the corrosion inhibition efficiency of DAN and DBN was excellent. The adsorption of inhibitors on the aluminum alloy surface followed Langmuir adsorption isotherms. Morphology observation revealed that the aluminum alloy was greatly protected by these triazinedithiol inhibitors. Further, density functional theory (DFT) was used to investigate the relationships between molecular structural and inhibition efficiency.

Keywords: aluminum alloy; potentiodynamic polarization; corrosion inhibition

1. Introduction

Corrosion of aluminum and its alloys has attracted much attention from many researchers due to their high mechanical intensity, low cost, low density, and good machinability, and they have been widely used in industrial applications, especially in constructions, electronics, packing, storage, and transportation equipment and machinery [1–6]. Corrosion is an electrochemical process and is often activated by industrial processes such as acid descaling, acid pickling, acid cleaning, and oil well acidizing [7]. Efforts have been made to protect the integrity of the aluminum surface in an aggressive acid medium or other corrosive environment. In recent decades, the addition of inhibitors has been considered to be the most common approach to hinder the corrosion of aluminum [7–10].

Many organic compounds have been widely reported as corrosion inhibitors of aluminum in acid solution, such as aliphatic, aromatic amines, and nitrogen heterocyclic molecules [11–15]. However, some of these compounds are costly and not easily biodegradable. As high reactive, low cost, high solubility, and environmentally friendly compounds, triazinedithiol, and its monosodium salt have been reported to prepare the effective corrosion inhibitive film on metal surfaces by electrochemical deposition [16–19]. The special tautomer of thiol–thione with highly electronegative atoms like S and O, and the N-containing heterocyclic conjugate system, benefit the triazinedithiol molecules to adsorb on metallic surface. However, the research on triazinedithiol inhibitors for aluminum alloy is seldom reported. The purpose of present work is to investigate and compare the corrosion inhibition action of 6-diallylamino-1,3,5-triazine-2,4-dithiol monosodium (DAN) and 6-dibutylamino-1,3,5-triazine-2,4-dithiolmonosodium (DBN), and their protective performance for

aluminum alloy (AA5052) in 1 M HCl was studied utilizing a variety of electrochemical tests, weight loss methods, scanning electron microscopy (SEM) techniques, and quantum chemistry analysis.

2. Materials and Methods

2.1. Materials and Sample Preparation

The aluminum alloy sheet AA5052 (Cu: 0.1%, Si: 0.2%, Fe: 0.4%, Mn: 0.1%, Mg: 2.8%, Zn: 0.1%, Cr: 0.3%, others: 0.15%) was mechanically press-cut into specimens of dimension 30 mm × 50 mm × 0.3 mm. All test plates of AA5052 were ultrasonically degreased in the acetone for 15 min, and treated by the immersion in alkaline solution (15 g Na_2CO_3 + 15 g Na_2PO_4 per liter) at 60 °C for the debinding process [20]. After that, the aluminum alloy specimens were washed thoroughly with distilled water and dried with nitrogen. The specimens with an exposed area of 1 cm^2 were used for potentiodynamic polarization and electrochemical impedance spectroscopy. AR (analytical reagent) grade hydrochloric acid and double distilled water were used to prepare the corrosive media. Molecular structures of DAN and DBN are displayed in Figure 1. In this paper, DAN was synthesized by the reaction between 6-*N*,*N*-diallylamino-1,3,5-triazine-2,4-dichloride and NaSH, while DBN was synthesized by the reaction between 6-*N*,*N*-dibutylamino-1,3,5-triazine-2,4-dichloride and NaSH according to the method in previous studies [19].

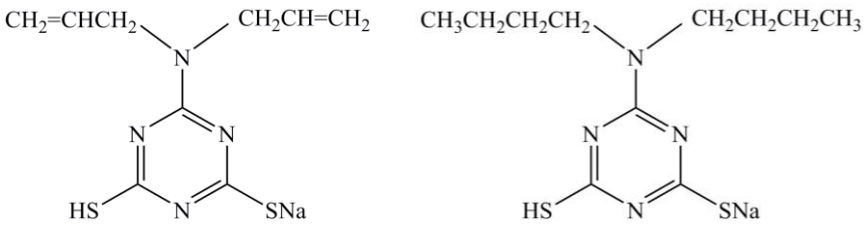

(**a**) (**b**)

Figure 1. Molecule structures of two triazinedithiols of (**a**) 6-diallylamino-1,3,5-triazine-2,4-dithiol monosodium (DAN) and (**b**) 6-dibutylamino-1,3,5-triazine-2,4-dithiol monosodium (DBN).

2.2. Weight Loss Test

The aluminum alloy specimens in triplicate were immersed in a 1 M HCl solution with different concentration (0.01–1.00 mM) of inhibitors for 2 h. The temperature was controlled by a thermostat aqueous bath at 30 °C. Furthermore, the aluminum alloy specimens were immersed into a 1 M HCl solution with the presence of 1 mM inhibitors, and the experiments were conducted over the temperature range from 30 °C to 50 °C. For all weight loss tests, the volume of prepared solution is 200 mL, and buffer solutions of citric acid/sodium citrate were used to adjust the pH value of tested solution between 6 and 6.5. After the immersion, all specimens were brought out from the solution, scrubbed with bristle brush under running water, then washed thoroughly with distilled water, dried in acetone, and weighed accurately. At least three samples were tested and the average value was obtained. The corrosion rates (C_R $g{\cdot}m^{-2}{\cdot}h^{-1}$) and inhibition efficiency (η_w %) were determined from the following equations:

$$C_R = \frac{W_0 - W_i}{ST} \quad (1)$$

$$\eta_w = \frac{C_R^0 - C_R^i}{C_R^0} \times 100 \quad (2)$$

where S is the area of aluminum alloy specimen (m^2); T is the exposure time (h); W_0 and W_i are the weight loss value in the absence and presence of inhibitor. C_R^0 and C_R^i are the corrosion rate ($g \cdot m^{-2} \cdot h^{-1}$) in the absence and presence of inhibitor molecules, respectively.

2.3. Electrochemical Measurements

The potentiodynamic polarization and electrochemical impedance spectroscopy (EIS) measurements were carried out using CHI 660C electrochemical work station (CHI Instruments; Shanghai, China) in a three-electrode cell system with a saturated calomel electrode (SCE) as reference electrode and a rectangular piece of graphite as counter electrode. The working electrode was AA5052. Prior to any electrochemical measurements, the immersion in the solution for 1 h was necessary for the open circuit potential to reach a steady state. EIS was carried out at steady open circuit potential disturbed with amplitude of 10 mV alternative current sine wave in the frequency range of 100 mHz to 10 kHz. The polarization curves were obtained by changing potential from −250 mV to +250 mV versus OCP with a scan rate of 0.5 mV/s.

2.4. Scanning Electron Microscopy (SEM)

The surfaces morphologies of the aluminum alloy immersed in a 1 M HCl solution for 2 h with and without the triazinethiol inhibitors were observed via SEM (JSM-6360LV, JEOL, Tokyo, Japan) at an accelerating voltage of 20 kV, respectively.

2.5. Quantum Chemical Calculation

Theoretical calculations were performed using DFT (density functional theory) at B3LYP/6-31G (d, p) basis set level with Gaussian 03 program [20]. Complete geometrical optimizations of DAN and DBN molecules structure, the highest occupied molecular orbital (HOMO), and the lowest unoccupied molecular orbital (LUMO) were obtained by using Gauss View. Some main quantum chemical indexes such as energy of HOMO (E_{HOMO}), energy of the LUMO (E_{LUMO}), and energy gap ΔE_{gap} between E_{HOMO} and E_{LUMO} were calculated and discussed.

3. Results

3.1. Weight Loss Study

3.1.1. Effect of Concentration

The inhibition efficiency (η_w) and corrosion rate (C_R) of aluminum alloy acquired from the weight loss method in a 1 M HCl solution contained different concentrations of inhibitors (0.01–1.00 mM) at 30 °C are presented in Table 1. The results clearly show that the inhibition efficiency increases and the corrosion rate decrease by increasing the concentration of studied inhibitors. When concentration of inhibitors varies from 0.01 mM to 1 mM, there is an increase in efficiency from 78.41% to 98.56% for DAN, and an increase in efficiency from 43.79% to 99.21% for DBN (Table 1). This suggests that the presence of DAN or DBN acts as inhibitor retarding the corrosion of aluminum in a hydrochloric acid solution. When the concentration of inhibitor is low, more molecules are needed to adequately cover the aluminum surface. We also found that further enhancement in concentration did not bring any significant changes in the performance of inhibitors, indicating that the achievement of a limiting value. The effect is attributed to the amassing of inhibitor molecules onto the positively charged metal surface leading a decrease in direct contact with metal and corrosive environment. Similar results were found in other studies about different inhibitors for aluminum alloy in hydrochloric acid [21].

Table 1. Corrosion parameters for aluminum alloy in a 1 M HCl solution with inhibitors concentrations range from 0.01 mM to 1.00 mM at 30 °C.

Conc.	DAN		DBN	
(mM)	C_R (g·m^{-2}·h^{-1})	η_w (%)	C_R (g·m^{-2}·h^{-1})	η_w (%)
Blank	90.90		82.15	
0.01	20.00	78.41	46.18	43.79
0.03	7.57	91.60	12.94	84.25
0.05	4.98	94.56	3.40	95.86
0.10	4.04	95.56	2.09	97.46
0.50	1.60	98.24	1.10	98.66
1.00	1.31	98.56	0.65	99.21

3.1.2. Effect of Temperature

Temperature has great influence on the corrosion rate of metals. The effect of solution temperature (30–50 °C) on corrosion rate and inhibition efficiency is shown in Figure 2. Compared with blank solution, the corrosion rate was significantly decreased in presence of inhibitors. It means that the addition of DAN and DBN compounds greatly inhibits the corrosion of aluminum alloy in 1 M HCl. The decrease in inhibition efficiency and increase in corrosion rate was observed with increase in temperature from 30 to 50 °C in the presence of 1 mM inhibitor, which may be attributed to the fact that the adsorption processes were spontaneous and irreversible with heat evolution, and the increase in temperature was not beneficial to the adsorption. The influence may also come from the weakening of electrostatic adsorption on the metal surface and the aggravation of desorption of the inhibitor molecule from the metal surface when the temperature increases [20–22]. In addition, the metallic corrosion in acidic environments is usually accompanied by the release of H_2, and the adsorption process of the inhibitor could be affected by the agitation caused by the acceleration of H_2 evolution rates at higher temperature and lead to the decrease of corresponding inhibition efficiency [23].

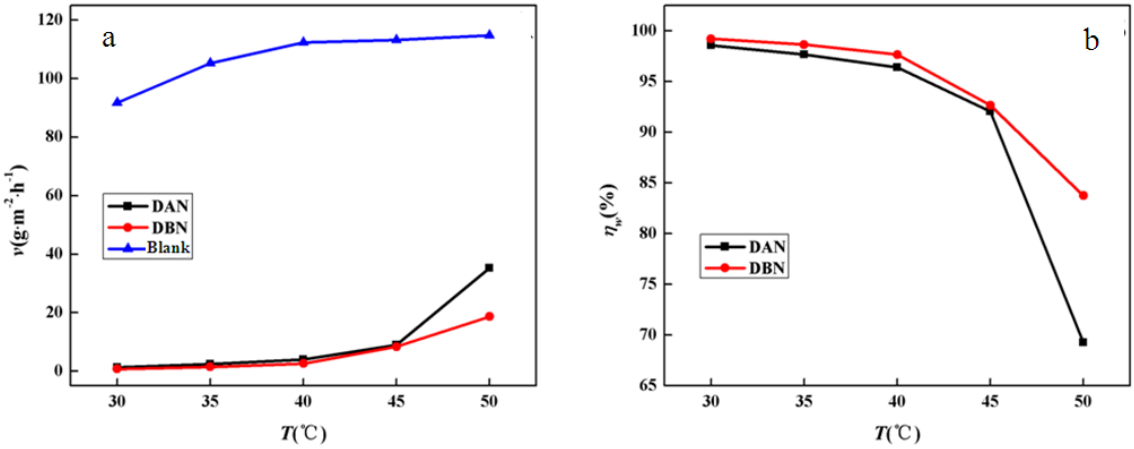

Figure 2. Variation of (**a**) corrosion rate and (**b**) inhibition efficiency of aluminum alloy in 1 M HCl with 1 mM inhibitor under different temperature (30–50 °C).

3.2. Electrochemical Measurements

3.2.1. OCP Measurement

Prior to each polarization or EIS experiment, the working electrodes were immersed in a 1 M HCl solution for 1 h to access the free corrosion potential or the quasi-stationary E_{oc} value. The plots of E_{oc} vs. time of AA5052 in the absence and presence of inhibitors for 1 h are given in Figure 3. For all test conditions, open circuit potential change (OCP) initially shifts fast towards a negative direction up

to 200 s. However, it shows a very slow decline for the rest of the experiment time and finally attains a steady value in approximately 1 h. The slight oscillations in OCP curves revealed that destruction and formation of corrosion product layer occurred at the metal surface [24]. The gradient shows that the surfaces of metals cannot achieve true steady states. In spite of this, the phenomenon indicates that there is a negligible change of OCP during the measurement period.

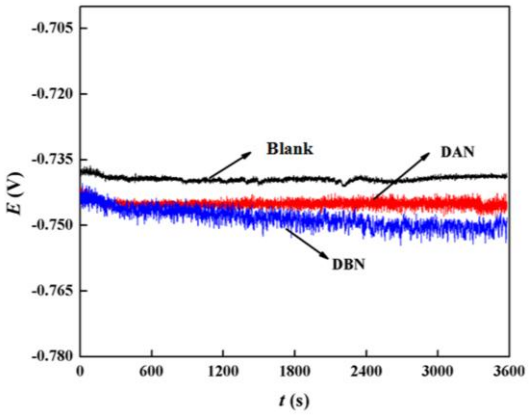

Figure 3. Open circuit potential change of AA5052 aluminum alloy in 1 M HCl without inhibitor (Blank) and with different inhibitors added (DAN or DBN), respectively.

3.2.2. Potentiodynamic Polarization

Potentiodynamic polarization profiles for AA5052 with different concentrations of DAN and DBN are presented in Figure 4. The corrosion kinetics parameters such as corrosion potential (E_{corr}), corrosion current density (I_{corr}), and cathodic and anodic Tafel slopes (β_a, β_c) were given in Table 2, where the inhibition efficiency η_p (%) was calculated by the following equation:

$$\eta_p(\%) = \frac{I^0_{corr} - I^i_{corr}}{I^0_{corr}} \times 100 \quad (3)$$

where I^0_{corr} and I^i_{corr} represent the corrosion current densities of AA5052 in the absence and the presence of inhibitor (DAN or DBN), respectively.

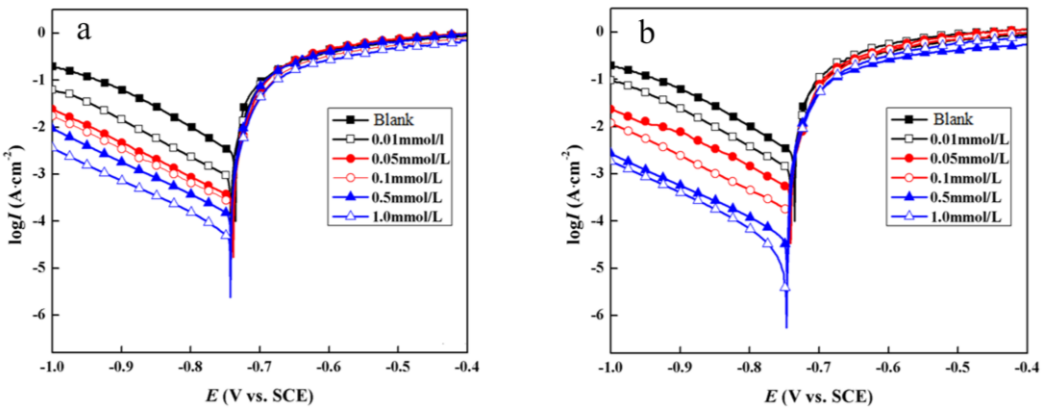

Figure 4. Tafel plots for aluminum alloy in 1 M HCl containing different concentrations of (**a**) DAN and (**b**) DBN.

Compared with the blank solution, the cathodic currents were significantly decreased with the presence of inhibitors and the addition of these compounds made E_{corr} shifted towards negative potentials (Figure 4), which suggested that DAN and DBN greatly reduced the hydrogen evolution

reaction, but their inhibition effects on the anodic dissolution were unobvious. Besides, the addition of DAN and DBN shift the cathodic and anodic curves to lower values, while the concentration of inhibitors was increased.

Table 2. Tafel polarization parameters of the corrosion for aluminum alloy in 1 M HCl containing different concentrations of DAN and DBN.

Inhibitor	C (mM)	E_{corr} (mV/SCE)	I_{corr} ($\mu A \cdot cm^{-2}$)	β_a ($mV \cdot dec^{-1}$)	β_c ($mV \cdot dec^{-1}$)	η_p (%)
	Blank	−735.90	2852.40	118.30	90.50	
DAN	0.01	−742.10	835.30	128.30	88.70	70.72
	0.05	−739.00	316.50	136.50	96.40	88.90
	0.10	−740.40	251.90	140.10	90.80	90.17
	0.50	−742.10	145.60	143.30	93.90	94.90
	1.00	−742.90	63.60	147.40	107.50	97.77
DBN	0.01	−740.40	1198.40	121.20	101.20	57.99
	0.05	−741.20	468.50	128.90	98.40	83.58
	0.10	−741.40	166.80	136.30	96.30	95.91
	0.50	−746.50	52.70	148.30	97.60	98.15
	1.00	−746.80	33.50	143.00	104.20	98.83

From Table 2, it is clearly seen that, when more inhibitors were added into the corrosive solution, the corrosion current density decreased and the inhibition efficiency increased. When the concentration of DAN or DBN reached 1 mM, the lowest I_{corr} values of 63.6 $\mu A \cdot cm^{-2}$ and 33.5 $\mu A \cdot cm^{-2}$ were obtained, and the inhibition efficiency achieved 97.77% and 98.83%, respectively. Generally, a compound is considered to anodic or cathodic type when the displacement in E_{corr} is greater than 85 mV; otherwise, inhibitor is considered as a mixed type [25]. For DAN and DBN, the E_{corr} values shift towards more a negative direction compared with the blank solution, but the change is not significant when the maximum displacement of E_{corr} values is 10.9 mV, which indicated that DAN and DBN belonged to mixed-type inhibitors, mainly inhibiting the cathodic processes.

3.2.3. Electrochemical Impedance Spectroscopy (EIS)

Nyquist plots for aluminum alloy in the absence and presence of various concentrations of DAN and DBN are given in Figure 5. The impedance spectra are consisted of capacitive loops at higher frequency and inductive loops at lower frequency. The presence of depressed semicircle in Nyquist plot across the studied frequency range indicates that a charge transfer process mainly controls the corrosion of aluminum. In other literature, similar plots have been reported for the corrosion of aluminum alloys in HCl solutions [20]. The inductive loop is generally attributed to the relaxation process in the oxide film covered on metal surface [26]. The reasons behind the deviations from perfect semicircles are usually involved with the frequency dispersion of interfacial impedance, which can be attributed to various kinds of physical phenomena such as active sites, surface roughness, and non-homogeneity of the solids [27]. The diameter of the capacitive loop is enlarging gradually with increasing concentrations of inhibitor, indicating that the charge transfer resistance is increased and the adsorbed inhibitor forms a more compact monolayer on metal surface with an increasing amount of inhibitor.

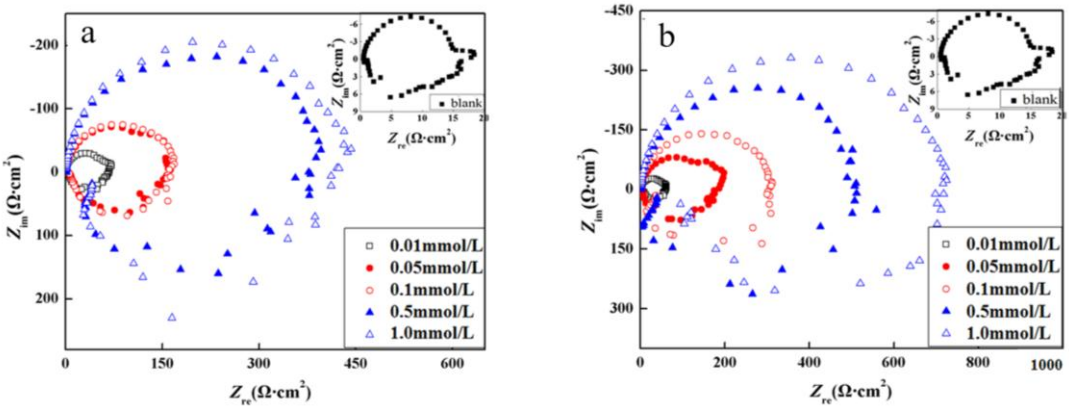

Figure 5. Nyquist diagrams for aluminum alloy in 1 M HCl containing different concentrations of (**a**) DAN and (**b**) DBN.

3.3. Surface Morphology

SEM technique was employed to further prove the corrosion resistance ability of DAN and DBN, and the surface observation images of aluminum alloy after a 2 h exposure in a HCl solution without and with inhibitors are shown in Figure 6. Before immersion, the bare aluminum plate looks very smooth (Figure 6a). In contrast, in the absence of inhibitor, the AA5052 presented a very rough surface covered with a huge amount of deep cracks and large holes, which suggests strong damage and a severe dissolution of aluminum alloy in contact with aggressive solution (Figure 6b). Nevertheless, in Figure 6c,d, the dissolution rate of aluminum alloy was substantially inhibited by DAN and DBN, exhibiting a comparative smooth surface with a few small pits. Therefore, it is concluded that the regular distribution of the DAN or DBN molecules adsorbed on AA5052 surface generates consistent protective layers, which effectively prevent HCl molecules from penetrating into the aluminum surface.

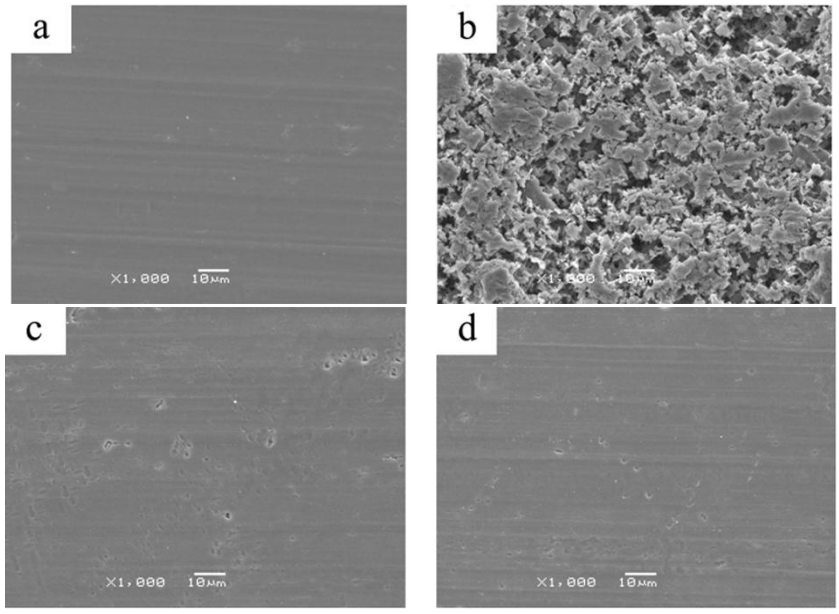

Figure 6. SEM images of AA5052 surface before and after immersing in 1 M HCl for 2 h without and with triazinedithiol inhibitors. (**a**) Blank before immersion; (**b**) blank after immersion; (**c**) with DAN; (**d**) with DBN.

3.4. Adsorption Isotherm

The interactions between the inhibitor molecules and the aluminum alloy surface can be investigated by adsorption isotherm [28]. To determine the adsorption mode, various isotherms including Langmuir, Frumkin, Temkin, and Freundlich were considered, and finally the Langmuir mode was found to be the most suitable adsorption isotherm. The linear relationships of C/θ versus C for DAN and DBN inhibitors are shown in Figure 7.

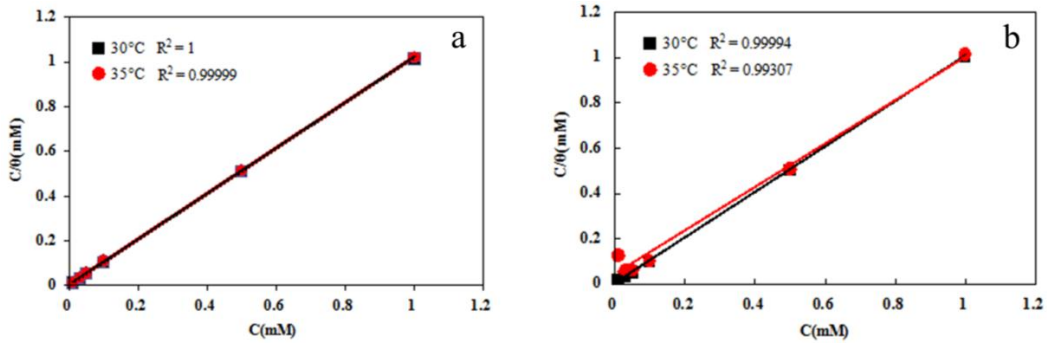

Figure 7. Langmuir isotherm adsorption isotherm of (**a**) DAN and (**b**) DBN in 1 M HCl solution.

The linear regression coefficients (R^2) are quite equal to 1, as shown in Figure 7, indicating that the adsorption of studied triazine derivatives on aluminum alloy surface obeys the Langmuir adsorption isotherm at 30 °C and 35 °C. The isotherm can be represented as follows:

$$\frac{c}{\theta} = \frac{1}{K_{ads}} + c \tag{4}$$

K_{ads} is the adsorptive equilibrium constant, c is the corrosion inhibitor concentration, and the fractional surface coverage θ can be easily calculated from the weight loss results (Table 1).

The equilibrium constants K_{ads} are related to the standard adsorption free energy (ΔG^{θ}) as shown in the following equation:

$$K_{ads} = \frac{1}{55.5}\exp\left(\frac{-\Delta G^{\theta}}{RT}\right) \tag{5}$$

where 55.5 (mol·L^{-1}) is molar concentration of water in solution, T (K) is the absolute temperature, and R (J·mol^{-1}·K^{-1}) is the molar gas constant. The K_{ads} and ΔG^{θ} values are given in Table 3. The negative values of ΔG^{θ} indicate that the inhibitor molecules are spontaneously adsorbed on the AA5052 surface to form a stable layer. In addition, the high K_{ads} value represents a strong adsorption of the inhibitor on aluminum alloy surface [29]. The strong interaction of inhibitors with aluminum alloy can be attributed to the presence of electronegative elements like nitrogen and sulfur, plus the π electrons on the triazine heterocyclic ring [30].

Table 3. Values of K_{ads} and ΔG^{θ} of DAN and DBN adsorbed on AA5052 at 30 °C and 35 °C.

Inhibitor	T (°C)	K_{ads} (L·mol^{-1})	ΔG^{θ} (kJ·mol^{-1})
DAN	30 °C	370,370	−42.4
	35 °C	136,990	−40.6
DBN	30 °C	169,490	−40.5
	35 °C	22,830	−36.0

In general, the ΔG^{θ} values of −40 kJ·mol^{-1} is accepted as threshold value between chemisorption and physisorption [30]. The ΔG^{θ} value more negative than −40 kJ·mol^{-1} may be indicative of the

sharing or transfer of electrons from the inhibitor molecules to the metal surface, while the value less negative than -20 kJ·mol^{-1} suggests a physisorption [31]. As mentioned above, it was concluded that the chemical adsorption was most possible for DAN at 30 °C or 35 °C and DBN at 30 °C based on the calculated ΔG^{θ} values of the present study displayed in Table 3. At 35 °C, the adsorption mechanism of DBN involves both physical and chemical processes with the calculated ΔG^{θ} value of -36 kJ/mol.

3.5. Quantum Chemical Calculation

Quantum chemical calculations have proven to be a very powerful tool for studying the corrosion inhibition mechanism. The optimized geometry of DAN and DBN are shown in Figure 8, and the main quantum chemical parameters are displayed in Table 4. It is observed that the electron densities of HOMO location in studied molecules are mostly distributed near the triazine heterocyclic rings, thiols, and the double bond between two carbons. It is well established in the literature that the E_{HOMO} often associated with the electron donating ability of a molecule. The high value of the HOMO energy is likely to indicate the tendency of a molecule to donate electrons to appropriate acceptor molecules with low-energy, empty molecular orbitals. Similarly, the value of E_{LUMO} reflects the ability of the molecule to accept electrons [32]. A molecule with a lower energy gap means a better inhibition ability, because the value of energy needed to remove an electron from the last occupied orbital is lower [33]. From Table 4, a higher E_{HOMO} value and lower energy gap were found in the DBN molecule, which demonstrated that DBN had an anti-corrosion capability superior to DAN. However, in the above experimental results, both DAN and DBN exhibited excellent corrosion performance, and the difference in inhibitive efficiency between them is not obvious. This may be related to the influence of their chemical structures. From Figure 8, we can find branched carbon chains in the DBN molecule structure that are longer than those of DAN. A larger space steric hindrance may influence the adsorption process of the inhibitor molecule [17], and the theoretical calculations that can only be a reference for the realities are usually more complex.

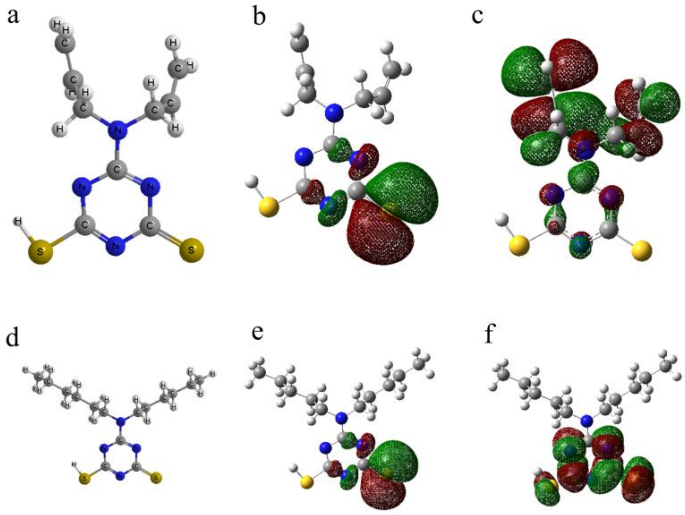

Figure 8. Frontier molecule orbital density distribution and optimized structures of DAN (a-structure; b-HOMO; c-LUMO) and DBN (d-structure; e-HOMO; f-LUMO).

Table 4. Quantum parameters for DAN and DBN [a].

Compound	E_{HOMO} (eV)	E_{LUMO} (eV)	ΔE_{gap} (eV)
DAN	−3.456	−0.789	2.667
DBN	−2.748	−0.844	1.904

[a] E_{HOMO} is energy of HOMO, E_{LUMO} is energy of LUMO, and $\Delta E_{gap} = E_{HOMO} - E_{LUMO}$.

4. Conclusions

Two triazinedithiol compounds (DAN and DBN) as corrosion inhibitors for aluminum alloy in a 1 M HCl solution were investigated. For DAN and DBN, their inhibition efficiency increased with increases in inhibitor concentration and they belonged to mixed-type inhibitors predominantly retarding the cathodic reaction. The inhibiting efficiencies determined by weight loss methods, potentiodynamic polarization testing, and EIS measurements are all in good agreement. The adsorption processes of DAN and DBN molecules followed the Langmuir adsorption isotherm. The calculated ΔG^{θ} values indicated that these inhibitors were spontaneously absorbed on the aluminum alloy surface and were more inclined to a chemisorption mechanism at 30 °C. The surface morphologies images were good proof for the reduction of dissolution of aluminum alloy ascribed to the formation of protective DAN/DBN film on the metal surface. In addition, the results were further verified by quantum chemical calculation, and these data support the good inhibition tendency of DAN and DBN.

Acknowledgments: The authors gratefully acknowledge the Fundamental Research Funds for the Central Universities (No. QN2013085) and the National Natural Science Foundation of China (No. 21203152).

Author Contributions: F.W. and Q.Z. conceived and designed the experiments; Q.Z. and T.T. performed the experiments; Q.Z. and F.W. wrote the paper; P.D. and Z.Z. modified the paper.

Conflicts of Interest: The authors declare no conflict of interest. The founding sponsors had no role in the design of the study; in the collection, analyses, or interpretation of data; in the writing of the manuscript; or in the decision to publish the results.

References

1. Dabalà, M.; Ramous, E.; Magrini, M. Corrosion resistance of cerium-based chemical conversion coatings on AA5083 aluminium alloy. *Mater. Corros.* **2004**, *55*, 381–386. [CrossRef]
2. Musa, A.Y.; Kadhum, A.A.H.; Mohamad, A.B.; Takriff, M.S.; Daud, A.R.; Kamarudin, S.K. On the inhibition of mild steel corrosion by 4-amino-5-phenyl-4H-1,2,4-trizole-3-thiol. *Corros. Sci.* **2010**, *52*, 526–533. [CrossRef]
3. Rosliza, R.; Nik, W.B.W.; Izman, S.; Prawoto, Y. Anti-corrosive properties of natural honey on Al–Mg–Si alloy in seawater. *Curr. Appl. Phys.* **2010**, *10*, 923–929. [CrossRef]
4. Hill, J.A.; Markley, T.; Forsyth, M.; Howlett, P.C.; Hinton, B.R.W. Corrosion inhibition of 7000 series aluminium alloys with cerium diphenyl phosphate. *J. Alloy. Compd.* **2011**, *509*, 1683–1690. [CrossRef]
5. Rosliza, R.; Nik, W.B.W.; Senin, H.B. The effect of inhibitor on the corrosion of aluminum alloys in acidic solutions. *Mater. Chem. Phys.* **2008**, *107*, 281–288. [CrossRef]
6. Gudić, S.; Vrsalović, L.; Kliškić, M.; Jerković, I.; Radonić, A.; Zekić, M. Corrosion inhibition of AA5052 aluminium alloy in 0.5 M NaCl solution by different types of honey. *Int. J. Electrochem. Sci.* **2016**, *11*, 998–1011.
7. Oguzie, E.E.; Onuoha, G.N.; Ejike, E.N. Effect of gongronema latifolium extract on aluminium corrosion in acidic and alkaline media. *Pigment Resin Technol.* **2007**, *36*, 44–49. [CrossRef]
8. Al-Turkustani, A.M.; Arab, S.T.; Al-Dahiri, R.H. Aloe plant extract as environmentally friendly inhibitor on the corrosion of aluminum in hydrochloric acid in absence and presence of iodide ions. *Mod. Appl. Sci.* **2010**, *4*, 105–124. [CrossRef]
9. Li, J.; Hurley, B.; Buchheit, R. Microelectrochemical characterization of the effect of rare earth inhibitors on the localized corrosion of AA2024-T3. *J. Electrochem. Soc.* **2015**, *162*, C563–C571. [CrossRef]
10. Ilevbare, G.O.; Scully, J.R. Mass-transport-limited oxygen reduction reaction on AA2024-T3 and selected intermetallic compounds in chromate-containing solutions. *Corrosion* **2001**, *57*, 134–152. [CrossRef]
11. Yurt, A.; Ulutas, S.; Dal, H. Electrochemical and theoretical investigation on the corrosion of aluminium in acidic solution containing some Schiff bases. *Appl. Surf. Sci.* **2006**, *253*, 919–925. [CrossRef]
12. Maayta, A.K.; Al-Rawashdeh, N.A.F. Inhibition of acidic corrosion of pure aluminum by some organic compounds. *Corros. Sci.* **2004**, *46*, 1129–1140. [CrossRef]
13. Khaled, K.F. Electrochemical investigation and modeling of corrosion inhibition of aluminum in molar nitric acid using some sulphur-containing amines. *Corros. Sci.* **2010**, *52*, 2905–2916. [CrossRef]
14. Zhang, Q.B.; Hua, Y.X. Corrosion inhibition of aluminum in hydrochloric acid solution by alkylimidazolium ionic liquids. *Mater. Chem. Phys.* **2010**, *119*, 57–64. [CrossRef]

15. Hachelef, H.; Benmoussat, A.; Khelifa, A.; Athmani, D.; Bouchareb, D. Study of corrosion inhibition by Electrochemical Impedance Spectroscopy method of 5083 aluminum alloy in 1 M HCl solution containing propolis extract. *J. Mater. Environ. Sci.* **2016**, *7*, 1751–1758.
16. Zhao, Q.; Tang, T.; Dang, P.; Zhang, Z.; Wang, F. Preparation and analysis of complex barrier layer of heterocyclic and long-chain organosilane on copper alloy surface. *Metals* **2016**, *6*, 162. [CrossRef]
17. Yoo, S.H.; Kim, Y.W.; Chung, K.; Kim, N.K.; Kim, J.S. Corrosion Inhibition Properties of Triazine Derivatives Containing Carboxylic Acid and Amine Groups in 1 M HCl Solution. *Ind. Eng. Chem. Res.* **2013**, *52*, 10880–10889. [CrossRef]
18. Li, Y.; Wang, D.; Zhang, H.; Wang, F. Study on triazinethiol electropolymerized films prepared by cyclic voltammetry and galvanostatic on copper alloy surface. *Int. J. Electrochem. Sci.* **2011**, *6*, 4404–4410.
19. Wang, F.; Liu, J.; Li, Y.; Fan, R. Complex barrier layer of triazinedithoil prepared by electrodeposition and initiated polymerization on aluminum alloy towards corrosion protection. *Int. J. Electrochem. Sci.* **2012**, *7*, 3672–3680.
20. Shalabi, K.; Abdallah, Y.M.; Fouda, A.S. Corrosion inhibition of aluminum in 0.5 M HCl solutions containing phenyl sulfonylacetophenoneazo derivatives. *Res. Chem. Intermed.* **2014**, *41*, 4687–4711. [CrossRef]
21. Obi-Egbedi, N.O.; Obot, I.B. Inhibitive properties, thermodynamic and quantum chemical studies of alloxazine on mild steel corrosion in H_2SO_4. *Corros. Sci.* **2011**, *53*, 263–275. [CrossRef]
22. Eddy, N.O.; Momoh-Yahaya, H.; Oguzie, E.E. Theoretical and experimental studies on the corrosion inhibition potentials of some purines for aluminum in 0.1 M HCl. *J. Adv. Res.* **2015**, *6*, 203–217. [CrossRef] [PubMed]
23. Halambek, J.; Jukić, M.; Berković, K.; Vorkapić-Furač, J. Investigation of novel heterocyclic compounds as inhibitors of Al-3Mg alloy corrosion in hydrochloric acid solutions. *Int. J. Electrochem. Sci.* **2012**, *7*, 1580–1601.
24. Schorr, M.; Yahalom, J. The significance of the energy of activation for the dissolution reaction of metal in acids. *Corros. Sci.* **1972**, *12*, 867–868. [CrossRef]
25. Kabir, K.B.; Mahmud, I. Study of erosion-corrosion of stainless steel, brass and aluminum by open circuit potential measurements. *J. Chem. Eng.* **2010**, *25*, 13–17. [CrossRef]
26. Abiola, O.K.; Otaigbe, J.O.E. Effect of common water contaminants on the corrosion of aluminium alloys in ethylene glycol–water solution. *Corros. Sci.* **2008**, *50*, 242–247. [CrossRef]
27. Maghraby, A.A.E. Corrosion inhibition of aluminum in hydrochloric acid solution using potassium iodate inhibitor. *Open Corros. J.* **2009**, *2*, 189–196. [CrossRef]
28. Ladha, D.G.; Wadhwani, P.M.; Kumar, S.; Shah, N.K. Evaluation of corrosion inhibitive properties of trigonellafoenum-graecum for pure aluminium in hydrochloric acid. *J. Mater. Environ. Sci.* **2015**, *6*, 1200–1207.
29. Şafak, S.; Duran, B.; Yurt, A.; Türkoğlu, G. Schiff bases as corrosion inhibitor for aluminium in HCl solution. *Corros. Sci.* **2012**, *54*, 251–259. [CrossRef]
30. Oguzie, E.E.; Li, Y.; Wang, F.H. Corrosion inhibition and adsorption behavior of methionine on mild steel in sulfuric acid and synergistic effect of iodide ion. *J. Colloid Interface Sci.* **2007**, *310*, 90–98. [CrossRef] [PubMed]
31. Herrag, L.; Hammouti, B.; Elkadiri, S.; Aouniti, A.; Jama, C.; Vezin, H. Adsorption properties and inhibition of mild steel corrosion in hydrochloric solution by some newly synthesized diamine derivatives: Experimental and theoretical investigations. *Corros. Sci.* **2010**, *52*, 3042–3051. [CrossRef]
32. Fouda, A.S.; Mohamed, F.S.; El-Sherbeni, M.W. Corrosion inhibition of aluminum–silicon alloy in hydrochloric acid solutions using carbamidic thioanhydride derivatives. *J. Bio- Tribo-Corros.* **2016**, *2*, 1–16. [CrossRef]
33. Kathirvel, K.; Thirumalairaj, B.; Jaganathan, M. Quantum chemical studies on the corrosion inhibition of mild steel by piperidin-4-one derivatives in 1 M H_3PO_4. *Open J. Met.* **2014**, *4*, 73–85. [CrossRef]

© 2017 by the authors; licensee MDPI, Basel, Switzerland. This article is an open access article distributed under the terms and conditions of the Creative Commons Attribution (CC BY) license (http://creativecommons.org/licenses/by/4.0/).